Available online at www.sciencedirect.com

SciVerse ScienceDirect

journal homepage: www.elsevier.com/locate/issn/15375110

Research Paper

# Estimating the plant stem emerging points (PSEPs) of sugar beets at early growth stages

*Henrik S. Midtiby**, *Thomas M. Giselsson*, *Rasmus N. Jørgensen*

*Institute of Chemical Engineering, Biotechnology and Environmental Technology, University of Southern Denmark, Niels Bohrs Allé 1, 5230 Odense M, Denmark*

ARTICLE INFO

*Article history:*
Received 11 February 2011
Received in revised form
12 October 2011
Accepted 31 October 2011
Published online 21 November 2011

Successful intra-row mechanical weed control of sugar beet (*beta vulgaris*) in early growth stages requires precise knowledge about location of crop plants. A computer vision system for locating plant stem emerging point (PSEP) of sugar beet in early growth stages was developed and tested. The system is based on detection of individual leaves; each leaf location is then described by centre of mass and petiole location. After leaf detection were the true PSEP locations annotated manually and a multivariate normal distribution model of the PSEP relative to the located leaf was built. From testing the system, PSEP estimates based on a single leaf have an average error of ~3 mm. When several leaves are detected the average error decreases to less than 2 mm.



## 1. Introduction

Mechanical inter-row weeding between crop rows has been used for a long time. However, mechanical intra-row weeding within rows between the single crop plants is relatively new. Physical intra-row methods can, in general, rely on three different strategies (Griepentrog & Dedousis, 2010: chap. 11): (1) soil coverage of weeds or (2) weed root/stem cutting or (3) uprooting of weeds (whole plant or partly). The first option is only relevant in some crop types such as cereals and potatoes. Sugar beet (*beta vulgaris*) at dicotyledon stage does not belong to these groups (Kouwenhoven, 1997; Melander, 2000) and only strategy (2) and (3) may be used.

Several intra-row mechanical weed management methods need to know where the crop plants are located, especially with concern to the plant stem emerging point (PSEP) which is defined as the point where the plant stem emerges from the soil surface. Computer vision was used by Tillett, Hague, Grundy, and Dedousis (2008) to locate transplanted cauliflower plants, before a cultivation disc was used so that the crop plants were not harmed. RTK-GPS has been used to mark the position of crop seeds during sowing (Griepentrog, Nørremark, Nielsen, & Blackmore, 2005), but the PSEP is not identical to the planted seed position, as the orientation of the seed is not taken into account. Nørremark, Griepentrog, Nielsen, and Søgaard (2008) used RTK-GPS coordinates to control a cycloid hoe doing intra-row weed control based on seed positions. Uncertainty in seed orientation, PSEP, and GPS accuracy limited the achievable precision to approx 30 mm. Sun et al. (2010) used RTK-GPS for mapping transplanted tomatoes; 95% of the plants were within 51 mm from the true plant position. Based on vision input crop plant positions may be determined with a higher accuracy and precision as Åstrand and Baerveldt (2002) indicated by guiding an autonomous weed robot with 20 mm accuracy along crop rows. Earlier work on extraction of individual leaves from images included that of Franz, Gebhardt, and Unklesbay (1991) which analysed boundary curvature by comparing with a known leaf shape and Neto, Meyer, and Jones (2006) which detected individual leaves in complex scenes based on

* *Corresponding author*. Tel.: +45 21356105.
E-mail address: hemi@kbm.sdu.dk (H.S. Midtiby).
1537-5110/$ – see front matter © 2011 IAgrE. Published by Elsevier Ltd. All rights reserved.
doi:10.1016/j.biosystemseng.2011.10.011

**Symbols and description**

| | |
|---|---|
| $\vec{S}$ | Petiole location, mm |
| $\vec{C}$ | Leaf centre of mass, mm |
| $\vec{z}_k$ | List of boundary coordinates, mm |
| $k$ | Index variable |
| $\Delta$ | Smoothing length |
| $l$ | Temporary distance threshold, mm |
| $\vec{x}_{lc}$ | Average PSEP location in plant frame, mm |
| $\Sigma_{1c}$ | Covariance matrix of PSEP location in plant frame, $mm^2$ |
| $\chi^2_{2,\alpha}$ | Chi square distribution with two degrees of freedom at the level 1 - $\alpha$ |
| x,y | Coordinate in plant frame, mm |
| $P_A(\vec{x}), P_B(\vec{x}), P_C(\vec{x})$ | Probability distribution of PSEP location in global frame, $mm^{-2}$ |
| $\vec{x}^A_c, \vec{x}^B_c, \vec{x}^C_c$ | Average PSEP location in global frame, mm |
| $\Sigma_A, \Sigma_B, \Sigma_C$ | Covariance of PSEP location in global frame, $mm^2$ |
| $D_1, \ldots, D_6$ | Sets of PSEP estimates produced by different methods |

*Abbreviations*

| | |
|---|---|
| MR | Missed root |
| BBCH | Growth stage classification scheme by Biologische Bundesanstalt, Bundessortenamt and chemical industry |
| FP | False positive |
| PSEP | Plant stem emerging point |
| RTK-GPS | Real time kinematics GPS |
| GPS | Global positioning system |
| NDVI | Normalised difference vegetation index |

Gustafson–Kessel clustering. This paper describes and evaluates a vision based method which detects single crop leaves and predicts where the corresponding PSEP is located.

## 2. Materials and methods

The current work consists of three parts: (1) development of a leaf detector, (2) building of a relative PSEP model, and (3) using the relative PSEP model to predict true PSEP based on detected leaves. An example image of sugar beet plants in early growth stages is shown in Fig. 1. The leaves can be described as convex objects with a thin stem (petiole). Leaves are detected by locating convex regions of the plant contour. The relative PSEP model is generated by comparing manually marked PSEP locations (i.e. ground truth values) with the detected leaves. Based on the relative PSEP location model and detected leaves, estimates of the true PSEP locations are obtained automatically. Finally, the methods for evaluating performance are described.

### 2.1. *Image acquisition and segmentation*

Images from sugar beet fields were acquired using a bi-spectral line scanning camera mounted on the Robovator (Poulsen, 2010) intra-row mechanical weeding robot. The setup for image capturing is shown in Fig. 2. The imaged sugar beet plants were part of field emergence trials conducted by Maribo Seed, Højbygårdvej 31, 4960 Holeby, Denmark in 2009. Precise plant placement is not required for field emergence trials which can be seen directly in the acquired images where sugar beet plants are distributed randomly over the captured region. The plants were in growth stages BBCH10-14. The captured area was illuminated with two 55 W halogen lamps. Each line in the acquired image consists of 256 pixels and a typical data file consisted of approximately 13,000 scan lines. A single pixel measured approximately 1.1 mm × 1.1 mm. A sample image can be seen in Fig. 1. For each pixel both a red and a near infrared value were available. Combining red and near infrared values makes it possible to segment images into plant material and soil which was done by calculating the normalised difference vegetation index (NDVI) value for each pixel (Backes & Jacobi, 2006). After this operation a single channel image was obtained with plant material having a high NDVI value compared to soil. This image is segmented using a threshold of 0.2 to form a binary image, the threshold was found by trial and error. These binary images are the basis for the data material used in this paper. Before further analysis the connected components are located. It was assumed that a leaf will only contribute to one connected blob. To remove noise, only blobs with areas larger than 160 pixels were kept.

### 2.2. *Leaf extraction*

For detecting leaves the general leaf structure was exploited. Examples of leaf shapes are shown in Fig. 1. The structure consisted of a large mainly convex region attached to the rest of the plant via a thin stem (petiole) (Meier, 2001). The leaf extraction method works in two steps. First convex regions are located and marked as leaf tip candidates; this is described in

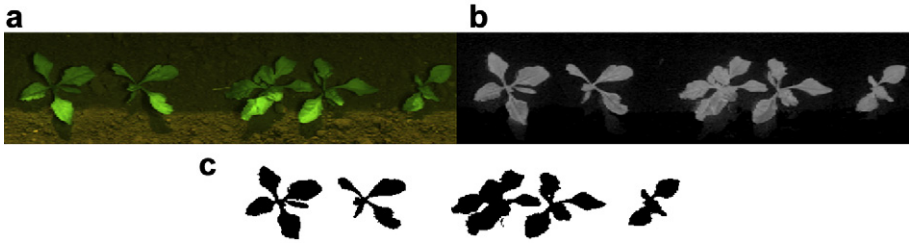


**Fig. 1 – Plant segmentation was done in two steps. First were NDVI values calculated for each pixel, then was the image thresholded. The shown images are (a) pseudo RGB image of raw data (red is shown as red and NIR is shown as green while the blue channel is set to zero) (b) NDVI image before thresholding and (c) after thresholding.**

Section 2.3. From the located leaf tip candidate a search for the corresponding petiole is then initiated, the search process is described in Section 2.4. If a petiole was located a leaf was found. When a leaf was detected the leaf location and orientation was described by petiole location $\vec{S}$ and the leaf centre of mass $\vec{C}$.

### 2.3. *Leaf tip candidate location*

Leaf tip candidates were found at local curvature minima in curvature of the plant boundary. At this stage the plant boundary was specified as the list of coordinates $\vec{z}_k$ where $k \in [1,\ldots,n]$ and the boundary was followed in a clockwise direction. The curvature was then defined as the angle between the line connecting point $k-\Delta$ and $k$ and the line connecting point $k$ and $k+\Delta$. The sign of the direction change indicated whether the current location of the boundary was concave or convex. The parameter $\Delta = 12$ was used together with a running average of the five nearest points. Plant boundary and curvature along the boundary was visualised in Fig. 3. Local maxima corresponds to concave regions, which were often located at leaf intersections or near the sugar beet growth point, which was assumed to be vertically above PSEP where several leaves are connected to a common area. Local minima corresponded to convex regions such as leaf tips.

To locate a candidate single leaf tip for each leaf, the following steps were used: (1) division of the boundary into concave and convex regions, (2) location of the minima in each convex region and (3) thresholding of the located minima. The purpose of the first step was to split the boundary into segments that at most contained a single leaf tip. Splitting points were used as locations where the curvature changes from positive to negative or from negative to positive values. The second step found the most likely leaf tip location, which were the points along the boundary where the boundary was convex and the change of direction was maximised. Step three removed possible leaf tip locations according to change of direction, if the change of direction was too small (i.e. less than 1 radians) the candidate was eliminated.

**Fig. 2 – The camera unit consisted of camera combined with halogen lamp. During image acquisition were eight such units mounted in front of a tractor.**

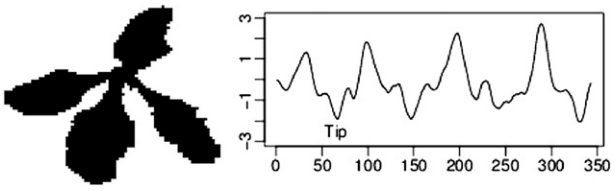


**Fig. 3 – Example of plant boundary and the calculated curvature along the boundary. The boundary is followed clockwise. Leaf tips are local minima and locations near the PSEP corresponds to peaks.**

### 2.4. *Location of corresponding petiole*

From each of the candidate leaf tips a search for the corresponding petiole was then initiated. Two walkers were placed at the leaf tip with the goal of following the boundary in each direction, one clockwise and one counter-clockwise. The movement of the walkers was controlled such that they reached the petiole nearly simultaneously. Each walker was then moved forward until the next step along the boundary brought the Euclidean distance between the walker and the leaf tip point above the specified threshold distance $l$. The distance between the walkers was then measured. This process (walker movement and distance measurement) was repeated with increasing values of $l$. In Fig. 4 the search strategy is visualised. For each value of the distance threshold the corresponding circle was drawn together with the two walker locations.

To locate the petiole, the distance between the walkers was investigated as follows: (1) search for a narrow leaf region which initiated the region in which the petiole could be located followed by (2) a search for a broadening of the leaf width which ends the region in which the petiole could be found. This strategy was implemented as a state machine. The state machine started in the leaf tip state and remained

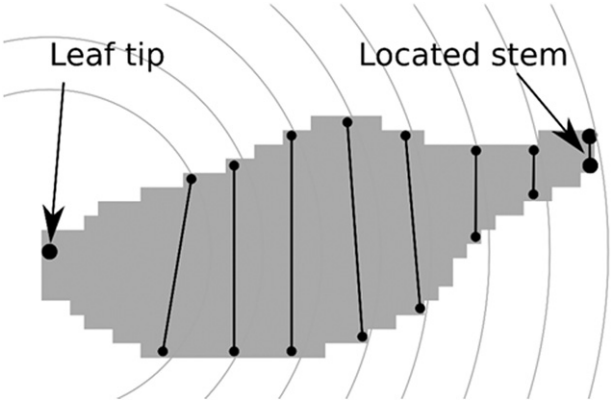


**Fig. 4 – Visualisation of the search strategy. The boundary was followed from the leaf tip until the Euclidean distance between the current location and the leaf tip exceeded a specified threshold. This was done in both directions and distance between the located points was measured. The procedure was repeated with increasing distance thresholds illustrated by concentric circles. When the distance between located points was minimised the leaf cut-off location was found.**

there until the distance between the two walkers got below half of the maximum distance between the walkers. At this point the state was changed to the leaf–stem state. In the leaf–stem state the system kept a track of the minimum distance between the walkers and corresponding walker locations. When the distance between the walkers exceeded three times the minimum distance observed in the leaf–stem state the search was terminated. The leaf boundary cut-off positions were given by the location of the walkers where the distance between the walkers was minimised within the leaf–state. The petiole location was set to the midpoint of the two boundary cut-off positions. To avoid infinite loops the petiole search was terminated if one of the walkers reached a leaf tip candidate or the two walkers passed each other.

### 2.5. Manual marking of root/leaf relative locations

After the automatic extraction of plant leaves, as described in Section 2.2, real PSEP locations were marked manually. A program showed each plant and the user then marked the pixel nearest the true PSEP. Fig. 5 illustrates a sample image with PSEPs marked with red spots and detected leaves marked by orange. To describe the marked PSEP location relative to the extracted leaf, the leaf coordinate system is placed with origin located at the petiole $\vec{S}$ and direction of the $x$ axis parallel to the vector $\vec{C} - \vec{S}$. An example is shown in Fig. 6.

The manual annotation of the location of the true PSEP locations was prone to errors. PSEP locations were marked with a single pixel, so the average quantisation error will be ~0.5 mm along each dimension. The true PSEP locations marked by an operator will also have an uncertainty. To estimate size of the typical error in this process the same image was annotated by two persons. Differences in PSEP locations were calculated and mean distance between annotations was determined.

### 2.6. PSEP location model

A multivariate normal distribution was used to model the PSEP location within the leaf coordinate system. The model was defined as:

$$p(\vec{x}) = \frac{1}{2\pi|\Sigma_{lc}|}\exp\left[\frac{-1}{2}(\vec{x} - \vec{x}_{lc})^T\sum_{lc}^{-1}(\vec{x} - \vec{x}_{lc})\right] \quad (1)$$

where $\vec{x}_{lc}$ is the centre of the true PSEP estimate and $\sum_{lc}$ is the covariance matrix. Both $\vec{x}_{lc}$ and $\sum_{lc}$ are expressed in the leaf coordinate system. Ellipses were used to visualise the multivariate normal distribution, contours of certain values are drawn such that a given fraction of the probability is inside the ellipses. To calculate the ellipses the formula below is used:

$$(\vec{x} - \vec{x}_{lc})^T\sum_{lc}^{-1}(\vec{x} - \vec{x}_{lc}) = \chi^2_{2,\alpha} \quad (2)$$

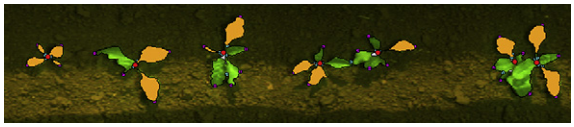

**Fig. 5 – Manually marking of PSEPs. The orange leaves were detected by the leaf detector. PSEPs are marked with red spots.**

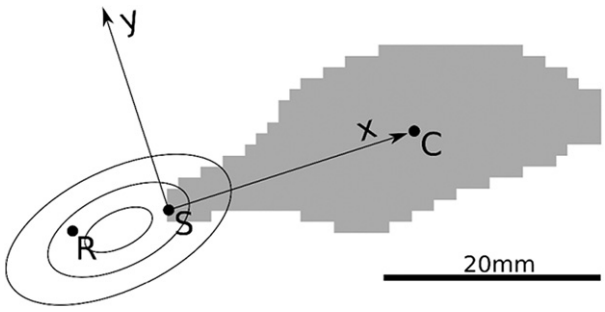


**Fig. 6 – PSEP location as specified in the leaf coordinate system. Where the centre of mass is C, stem attach point S and PSEP location R. The PSEP location model is indicated by the three concentric ellipses. According to the PSEP location model, 68% of the true PSEP locations will be placed within the central ellipse, the two other ellipses will contain 95% and 99.7% respectively.**

where $\chi^2_{2,\alpha}$ is the $\chi^2$ distribution with 2 degrees of freedom and $P$ value $1-\alpha$. Typical fractions used for visualisation are 68%, 95% and 99.7%. As the PSEP is defined relative to the leaf (Fig. 6) the $x$ and $y$ coordinate values were translated to a displacement along the major leaf axis and displacement perpendicular to the same axis respectively. The PSEP was expected to lie in extension of the primary leaf axis (low $y$ values) shifted to negative $x$ values. For later analysis position and uncertainty parameters were converted to the global coordinate system using a coordinate transformation based on rotation and translation.

### 2.7. Combination of relative PSEP location models

In many cases it is possible to detect more than a single leaf, an example is shown in Fig. 7. In the figure 99.7% ellipses of the two estimates of the true PSEP share a common region and it could be expected that the true PSEP was located within this region. To combine two PSEP models ($p_A(\vec{x})$ and $p_B(\vec{x})$) the probability densities are multiplied and normalised.

$$p_c(\vec{x}) \propto p_A(\vec{x}) \cdot p_A(\vec{x}) \quad (3)$$

If the PSEP models are defined by the parameters $\sum_A$,$\sum_B$, $\vec{x}_c^A$ and $\vec{x}_c^B$ the parameters of the combined model expressed as (Gales & Airey, 2006)

$$\sum_C^{-1} = \sum_A^{-1} + \sum_B^{-1} \quad (4)$$

$$\vec{x}_c^C = \sum_C\left(\sum_A^{-1}\vec{x}_c^A + \sum_B^{-1}\vec{x}_c^B\right) \quad (5)$$

This combination of PSEP models was based on the same principle as least squares estimation used in the Kalman filter.

### 2.8. Generation of position predictions

To test the developed method for PSEP estimation, the method was applied to a test image. True plant locations were determined manually and compared to six sets $D_{1,\ldots,6}$ of predicted PSEP locations. These sets were used to measure accuracy of

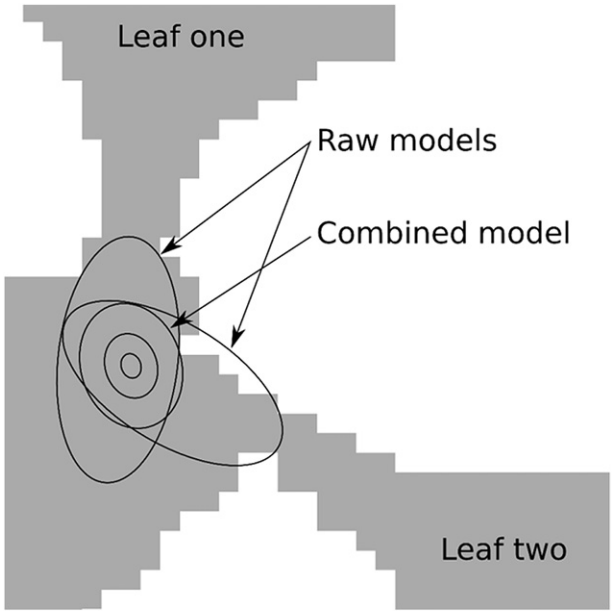


**Fig. 7 – Combination of two PSEP location models. The ellipses are similar to those shown in Fig. 6. For the raw models the ellipses for 99.7% are shown and for the combined model 68%, 95% and 99.7%, respectively.**

the located PSEPs under different conditions, eg. different number of detected leaves per plant.

From all the detected leaves a PSEP were generated (using only information from this leaf). This was a set $D_1$. $D_2$ containing PSEPs calculated from two detected leaves. All possible combinations were tested and leaf pairs were combined if distance between centres of their PSEP models was less than 20 mm. $D_3$ and $D_4$ were similar to $D_2$ except that 3 and 4 leaves are used for calculating the PSEP. For a plant where $n$ leaves were detected, the set $D_k$ would contain $\binom{k}{n}$ elements related to that plant. Not all plants had all four leaves detected, therefore they did not contain PSEPs associated to these plants. Thus the number of leaves used to calculate PSEPs increased, the precision of the located PSEPs increased, but a larger fraction was missed. $D_5$ was a compromise between large coverage and low placement error. The set was built on $D_1$ by merging PSEP models with a distance between predicted plant centres of 20 mm or less. This merging scheme generated combined PSEP models based on position information from up to 4 leaves. In addition was a set, $D_6$, generated by manual annotation by a different person than the one who marked the reference PSEPs. $D_6$ covered only one third of the test image and was used to estimate the uncertainty of the manually marked PSEPs.

### 2.9. *Performance evaluation*

Performance of the PSEP location models was judged according to the following values:

**False positives (FPs):** If a leaf was falsely found by the leaf separator method it constituted a FP. These cases were characterised by having a long distance from the predicted PSEP to the nearest true PSEP. FPs were detected by setting a threshold on the allowed distance from predicted leaf location to the nearest true PSEP.

**Missed PSEP locations:** If none of a plant's leaves were detected a PSEP was missed. It was characterised by having a long distance from the true PSEP to the nearest predicted PSEP. Missed PSEPs were detected by setting a threshold on the allowed distance.

**Predicted position error:** The errors in the predicted PSEP location were averaged for all predicted PSEP locations with an error less than a threshold of 20 mm.

## 3. Results

### 3.1. *Leaf detector performance*

For evaluating performance of the leaf detector, the 805 leaves present in the test images were counted manually. The leaf detector located 46.6% (395) leaves, of those 2.4% (19) were FPs.

### 3.2. *Relative PSEP model*

The leaf detector was applied to three datasets. True PSEPs were marked by hand in all three datasets. Additionally leaves were detected by the leaf detector method and their location specific information recorded. Analysing leaves and PSEPs led to the generation of 223 data points. In the local leaf coordinate system the multivariate normal distribution model was described by the parameter values:

$$\vec{x}_{lc} = \begin{pmatrix} 5.40 \\ 0.24 \end{pmatrix} \text{mm} \qquad \sum_{lc} = \begin{pmatrix} 12.65 & 1.28 \\ 1.28 & 2.35 \end{pmatrix} \text{mm}^2 \tag{6}$$

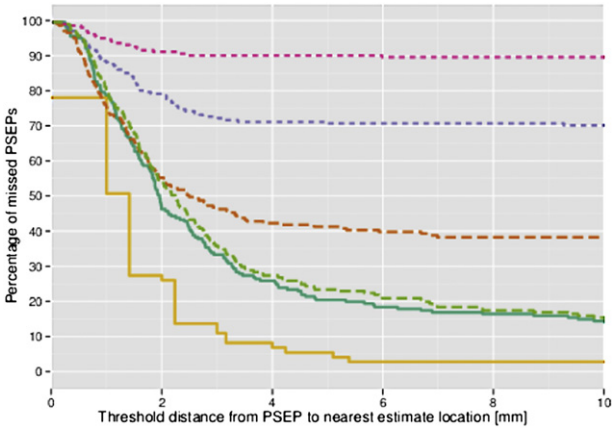


**Fig. 8 – Fraction of missed PSEPs as a function of the threshold distance. When the number of leaves used to estimate true PSEPs was increased, the fraction of missed PSEPs also increased. The following colour coding is used: D1: dashed green line, D2: dashed dark orange line, D3: dotted blue line, D4: dotted pink line, D5: green line and D6: orange line.**

**Table 1 – Performance statistics of the PSEP estimates. Count; number of position estimates. FP; false positives, percentage of predicted plant positions with a distance to the nearest true plant location larger than 20 mm. MR; missed roots, percentage of true PSEPs within 20 mm of a predicted PSEP location. Avg; average estimate error in mm. 95%; the 95% quantile of estimate errors in mm.**

| Set | Number of leaves | Count | FP | MR | Avg | 95% |
|---|---|---|---|---|---|---|
| $D_1$ | 1 | 395 | 4.8%(19) | 10.0% | $3.29 \pm 0.14$ | 15.76 |
| $D_2$ | 2 | 313 | 1.6%(5) | 37.3% | $1.88 \pm 0.07$ | 4.62 |
| $D_3$ | 3 | 132 | 0.8%(1) | 70.1% | $1.42 \pm 0.09$ | 3.02 |
| $D_4$ | 4 | 29 | 0.0%(0) | 89.1% | $1.22 \pm 0.20$ | 2.39 |
| $D_5$ | 1–4 | 188 | 8.0%(15) | 10.4% | $2.66 \pm 0.21$ | 49.51 |
| $D_6$ | na | 71 | 0.0%(0) | 2.7% | $1.37 \pm 0.26$ | 3.58 |

### 3.3. *Fraction of PSEP locations found*

The fraction of missed PSEPs was visualised as a function of the chosen threshold in Fig. 8. All six PSEP prediction methods showed the same trend. At first the fraction of missed PSEPs decreased linearly until the curve flattened out. The point where the curve flattened out indicated the maximum error of the position estimate and the fraction of PSEPs that were not found. Note that humans were good at locating a large fraction of the PSEPs. The fraction of roots not found within 20 mm is shown in the missed root (MR) column in Table 1. If a single leaf ($D_1$) was used to predict PSEPs, approximately 10% of the true PSEPs were missed, this number increased strongly when the number of leaves used in the prediction was increased. Approximately 37% of the true PSEPs were missed with estimates based on two leaves and this number increased to ~89% when four leaves were used to generate estimates. This increase in the fraction of missed PSEPs was only to be expected, as the plants with one or two detected leaves were not present in $D_3$ and $D_4$.

### 3.4. *Fraction of FPs*

To gain insight in the accuracy of PSEP location estimates the fraction of FPs was visualised as a function of threshold distance in Fig. 9. The figure was divided into four regions, each representing a dataset. Dataset *One* is the PSEP near which the leaf detector found a single leaf; *Three* is when the leaf detector located three leaves. From the green curve it is seen that ~20% of the $D_1$ position estimates had a distance (error) > 4 mm to the nearest true PSEP, for comparison the corresponding distance for $D_2$ was 3 mm. The figure shows that when the number of leaves used to generate a PSEP location estimate was increased the error in the estimate was reduced significantly. The figure was divided into four underlying datasets such that each dataset could be weighted appropriately. If all the data was shown in one plot it would have been difficult to interpret because each set of location estimates was based on a unique dataset. The number of FPs and MRs for each of the estimate sets is given in Table 1. The listed values were found using a threshold distance of 20 mm. In addition the estimate error (distance from estimate to nearest PSEP) was described using the average value and the 95% quantile (i.e. 95% of the predicted PSEP had an error of less than that value).

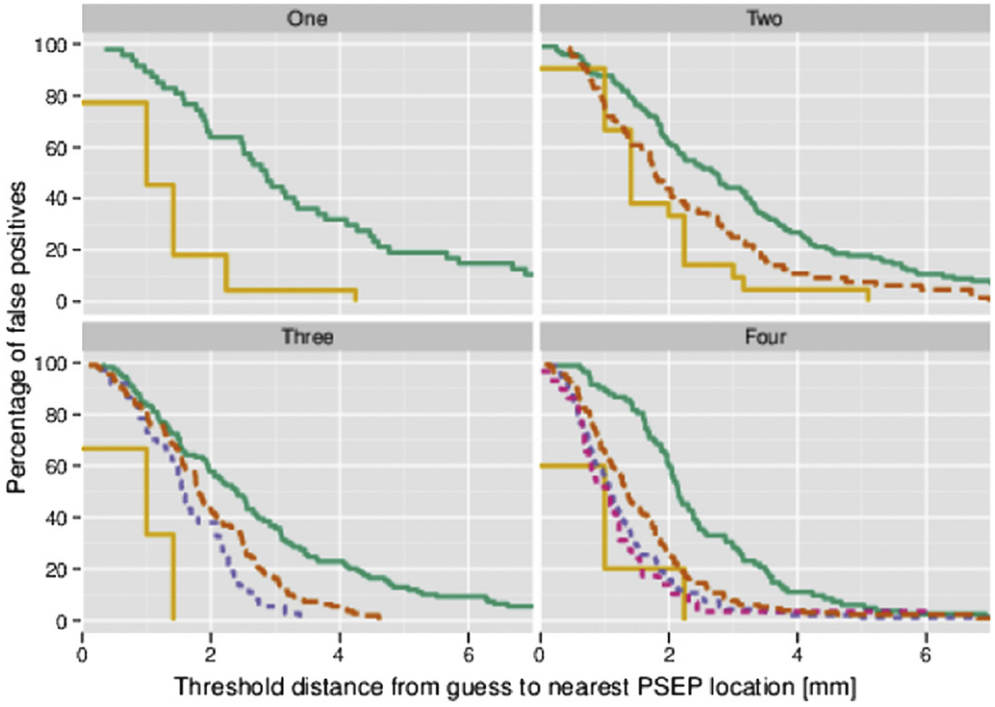


**Fig. 9 – Fraction of false positives as a function of the threshold distance. Error of PSEP location estimates was seen to decrease when the number of leaves used to make the estimate increased. Colour codings as in Fig. 8.**

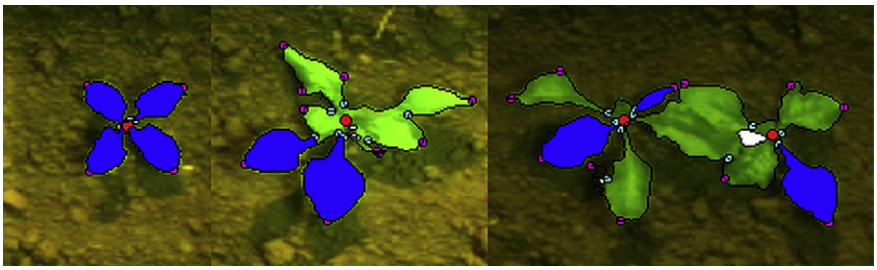

**Fig. 10 – Easy and difficult cases for the leaf detector. Leaf tip candidates are marked by purple squares. Cyan indicates concave locations. Detected leaves are marked in blue.**

## 4. Discussion

The leaf detector was not able to locate all leaves in the test images. This was due to overlapping leaves, leaves with irregular shapes and, to a certain extent, limitations in the implemented algorithm. Some typical cases are shown in Fig. 10. The petiole search was fragile and failed if more than a single leaf tip candidate was found in one leaf. In the used leaf definition (convex area with a thin petiole) overlapping leaves could have influenced both criteria: the combined leaf area was not guaranteed to be convex and the petiole region could have been hidden or widened. Rarely will the relative location of leaf tip estimate and petiole cause the petiole search strategy to fail; this is the case when the distance between petiole and leaf tip estimate is less than the distance between leaf tip estimate and the true leaf tip. To reduce the fraction of missed PSEPs the leaf detector must be improved. If a PSEP is not located none of the associated leaves have been detected.

Before evaluation of the implemented algorithms the uncertainty of the true PSEP position should be investigated. This can be achieved by comparing true PSEPs with PSEPs determined by a person different from the one who determined the true PSEPs initially. The difference between such two manual annotations can be used as an estimate of the position uncertainty of the true PSEPs. On average the difference was 1.37 mm and in 95% of the cases the difference between the two human annotations was $< 3.58$ mm. Two sources contributed to this difference (1) quantification errors and (2) the uncertainty / unreliability of the human annotation. The quantification error originated from the annotation program, which used integer coordinates to describe PSEPs. A rough estimate of this error is $\sim 0.5$ mm along the two coordinate axes. The human annotation unreliability originated from differences in test image interpretation.

When the leaf detector found two leaves of a single plant the corresponding true PSEP will, with a probability of 95%, be within a distance of 5 mm or less from the estimate. This and similar values are shown in Table 1. Sun et al. (2010) were able to measure the position of transplanted crops with an RTK-GPS unit within 51 mm for 95% of the plants. The accuracy of the vision system was therefore one order of magnitude better than RTK-GPS seeding of plants. When three or more leaves were used to predict PSEPs the accuracy was comparable to the human annotation. One interpretation of this is that the developed method can predict PSEPs with a higher accuracy than the reference predictions based on manual annotation given that two or more leaves are detected for each PSEP.

## 5. Conclusion

A system for automated PSEP estimation of sugar beet plants (in growth stages BBCH10-14) based on leaf detection has been developed and tested. In a set of test images the system detected 46.7% of the present leaves. A multivariate Gaussian PSEP model was built based on the detected leaves and manual annotation of true PSEPs. Given centre of mass and attach point of a single leaf the model stated that the average true PSEP was at a distance of 6.2 mm from the petiole attachment point and placed on the line connecting the leaf attach point and the leaf centre of mass. Ninety-five % of the volume below the multivariate Gaussian was contained within an ellipse with semi-major and semi-minor axes of 12 mm and 6 mm respectively.

In the set of test images the detected leaves were used to predict the true PSEPs. With PSEP predictions based on single leaves 90% of the true PSEPs were located within 20 mm of at least one predicted PSEP location. In this case the average distance from the predicted location to the true PSEP was 3.3 mm. When several leaves of the same plant are detected, the PSEP models can be combined using least-squares estimation and thus produce an even better estimate of the true root location. For example, by combining two leaves the average error was reduced to 1.9 mm. Precise quantification of the error in three and four leaf based PSEP estimates is hindered as these methods performed on par with the human annotation used as reference.

## REFERENCES

Åstrand, B., & Baerveldt, A.-J. (Jul. 2002). An agricultural mobile robot with vision-based perception for mechanical weed control. *Autonomous Robots, 13*(1), 21–35. http://dx.doi.org/10.1023/A:1015674004201.

Backes, M., & Jacobi, J. (2006). Classification of weed patches in Quickbird images: verification by ground truth data. *EARSeL European Association of Remote Sensing Laboratories,* 5(2), 172–179. http://www.eproceedings.org/static/vol05_2/05_2_backes1%.html.

Franz, E., Gebhardt, M.Unklesbay, K. (1991). Shape description of completely visible and partially occluded leaves for identifying plants in digital images. 34. p. 673–681.

Gales, M., & Airey, S. (Jan. 2006). Product of Gaussians for speech recognition. *Computer Speech & Language, 20*(1), 22–40. http://

www.sciencedirect.com/science/article/B6WCW-4FBH%W7F-1/2/b1001c29af3057ecce30bfe8e9592955.

Griepentrog, H. W., & Dedousis, A. P. (2010). *Mechanical weed control, Vol. 20*. Heidelberg: Springer Berlin, 171–179.

Griepentrog, H. W., Nørremark, M., Nielsen, H., & Blackmore, B. S. (2005). Seed mapping of sugar beet. *Precision Agriculture, 6*, 157–165. doi:10.1007/s11119-005-1032-5. http://dx.doi.org/10.1007/s11119-005-1032-5.

Kouwenhoven, J. K. (1997). Intra-row mechanical weed control—possibilities and problems. *Soil and Tillage Research, 41*(1–2), 87–104. http://www.sciencedirect.com/science/article/B6TC6-3RGT%BJD-7/2/3ce3ed554667f0adfed53ebb227deeb6.

Meier, U. (2001). Growth stages of mono-and dicotyledonous plants. http://www.bba.de/veroeff/bbch/bbcheng.pdf.

Melander, B. (2000). Mechanical weed control in transplanted sugar beet. In: 4th EWRS Workshop on Physical Weed Control. http://orgprints.org/1542/1/Abstract_Elspeet1.pdf.

Neto, J. C., Meyer, G. E., & Jones, D. D. (Apr. 2006). Individual leaf extractions from young canopy images using Gustafson-Kessel clustering and a genetic algorithm. *Computers and Electronics in Agriculture, 51*(1–2), 66–85. http://www.sciencedirect.com/science/article/B6T5M-4J2M%44F-1/2/b947a39d2c204692a56e44750203ac42.

Nørremark, M., Griepentrog, H., Nielsen, J., & Søgaard, H. (2008). The development and assessment of the accuracy of an autonomous gps-based system for intra-row mechanical weed control in row crops. *Biosystems Engineering, 101*(4), 396–410. http://www.sciencedirect.com/science/article/B6WXV-4TX6%W5S-1/2/8aede62984cd66ed1ef62aa58e1518f3.

Poulsen, F. (2010). Measuring emerging plants using machine vision. http://www.visionweeding.com/Products/Plant-Counting/Plant-Counting.htm.

Sun, H., Slaughter, D. C., Ruiz, M. P., Gliever, C., Upadhyaya, S. K., & Smith, R. F. (Apr. 2010). Rtk gps mapping of transplanted row crops. *Computers and Electronics In Agriculture, 71*(1), 32–37.

Tillett, N., Hague, T., Grundy, A., & Dedousis, A. (2008). Mechanical within-row weed control for transplanted crops using computer vision. *Biosystems Engineering, 99*(2), 171–178. http://www.sciencedirect.com/science/article/B6WXV-4R5H%1V8-2/2/4487816230cc4673f885d6bd784c79a2.